JOC The Journal of Organic Chemistry

Article

pubs.acs.org/joc

Enantioselective Organocatalytic Intramolecular Diels–Alder Reactions: A Computational Study

Filipe J. S. Duarte and A. Gil Santos*

REQUIMTE, CQFB, Departamento de Química, Faculdade de Ciências e Tecnologia, Universidade Nova de Lisboa, 2829-516 Caparica, Portugal

Supporting Information

ABSTRACT: The diastereo- and enantioselectivity obtained experimentally by Christmann in the amine-catalyzed intramolecular Diels–Alder reaction of α,β-unsaturated carbonylic compounds were fully rationalized using density functional theory methods at the PBE1PBE/6-311+G** level. A polarizable continuum model was used to describe solvent effects. The selectivity is induced in the cyclization step, and while the enantioselectivity results from the *syn*/*anti* orientation around the C–N enamine bond, the diastereoselectivity mainly results from the *syn*/*anti* configuration of the substituents in the forming cyclopentane ring. The remarkable reaction rate experimentally observed when an external protic acid is used is attributed to the strong decrease in the activation energy of all steps needed for the enamine formation, while the external acid marginally influences the cyclization step. When hydrogen-bond-donor catalysts are used, the formation of one hydrogen bond in the cyclization step inverts the configuration and reduces the selectivity. The different behavior between dialdehydes and ketoaldehydes is suggested to be resulting from different reaction rates in the catalyst elimination step.

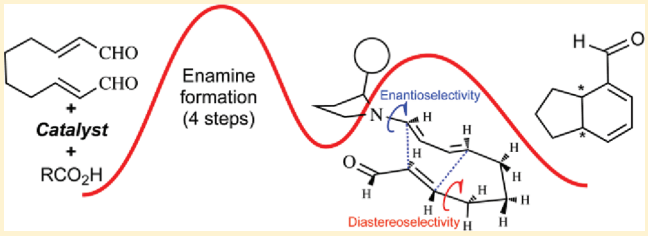

INTRODUCTION

Over the past decades, numerous studies on catalytic intermolecular asymmetric Diels–Alder reactions have been published, mainly involving the LUMO-lowering activation of electron deficient dienophiles, by the catalysis of either metal-based[1−3] or organic molecules.[4] In 2000, MacMillan et al. defined the general concept of activation of α,β-unsaturated carbonyl compounds with an external secondary amine catalyst (Scheme 1),[5] establishing that the LUMO-lowering activation of α,β-unsaturated carbonyl groups via the reversible formation of an iminium ion with an external amine catalyst is a valuable platform for the development of a variety of enantioselective cycloadditions,[5,6] Friedel–Crafts alkylations,[7,8] conjugate additions,[9] and hydrogenations.[10] More recently, in their seminal γ-amination work, Jørgensen and co-workers[11] reported the formation of cycloadduct **3** as a result of the Diels–Alder reaction between an electron-rich dienamine **1** and a maleimide **2** (Scheme 1). In this case, the HOMO–LUMO gap between the diene and the dienophile is reduced due to the high energy of the dienamine HOMO orbital. Thus, the enamine/imine formation can be used either to lower the LUMO of the dienophile or to prepare a dienamine with high HOMO energy.

Scheme 1. Diels–Alder Activation with Secondary Amines: (I) LUMO-Lowering Activation via the Reversible Formation of an Iminium Ion; (II) HOMO-Raising Activation by the Formation of an Electron-Rich Dienamine[11]

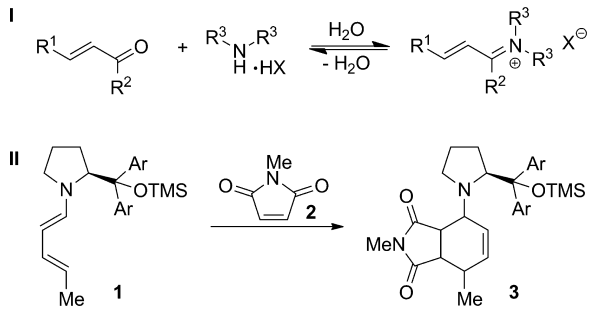

Although until recently only examples of asymmetric inverse-electron-demand hetereo-Diels–Alder reactions were known,[12−15] in 2010 Chen and co-workers have been able to implement the first known example of an all-carbon-based asymmetric organo-catalytic inverse-electron-demand intermolecular DA reaction.[16] Chen followed a similar approach to that used by Jørgensen,[11] but instead of using the dienamine as diene he used it as an electron-rich dienophile in a reaction with an electron-poor diene. Thus, the reaction occurs via the diene low energy LUMO orbital and the dienophile high energy HOMO orbital, as described in Scheme 2.

Supported by the good results obtained in the intermolecular processes, a few researchers focused their efforts on the intramolecular Diels–Alder (IMDA) variant. In recent years, several natural polycyclic compounds have been synthesized by

Received: January 2, 2012
Published: February 26, 2012

dx.doi.org/10.1021/jo300005e | J. Org. Chem. 2012, 77, 3252–3261

Scheme 2. Inverse-Electron-Demand Diels–Alder Reaction[16]

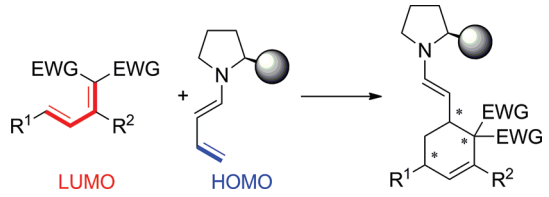

this approach, as the reaction provides ready access to these types of structures with outstanding stereoselectivity. Several useful drugs such as solanapyrone A[17] and D,[18] salvinorin A,[19] lepidopteran,[20] and himbacine[21] are examples of compounds whose complete synthesis was accomplished using the asymmetric catalyzed IMDA reaction, via the LUMO-lowering activation of electron deficient dienophiles.

Recently, and based on the previous results obtained by Jørgensen,[11] Christmann et al.[22] reported a methodology to prepare bicyclic compounds, with moderate to high stereoselectivity, by intramolecular Diels–Alder reaction of α,β-unsaturated carbonylic compounds, using the dienamine activation approach, which raises the diene HOMO energy (Scheme 3). Several catalysts were tested, the selectivity being dependent on the presence of hydrogen-bond donors. Changes in the substrate also influence the reaction outcome, as while dialdehydic compounds lead to cycloadducts, the presence of a keto group favors the formation of Michael adducts (Scheme 3).

In this paper, we computationally study the experimental results reported by Christmann et al. (Scheme 3),[22] aiming at a selectivity rationalization that can allow for the development of optimized reagents and catalysts.

RESULTS AND DISCUSSION

It is accepted that the amine-catalyzed IMDA reaction of dialdehydes follows an enamine pathway, as described in Scheme 4.[22] The enamine formation steps have been intensely

Scheme 4. Proposed[22] Mechanism for the IMDA Reaction of Dialdehydes Catalyzed by Secondary Amines

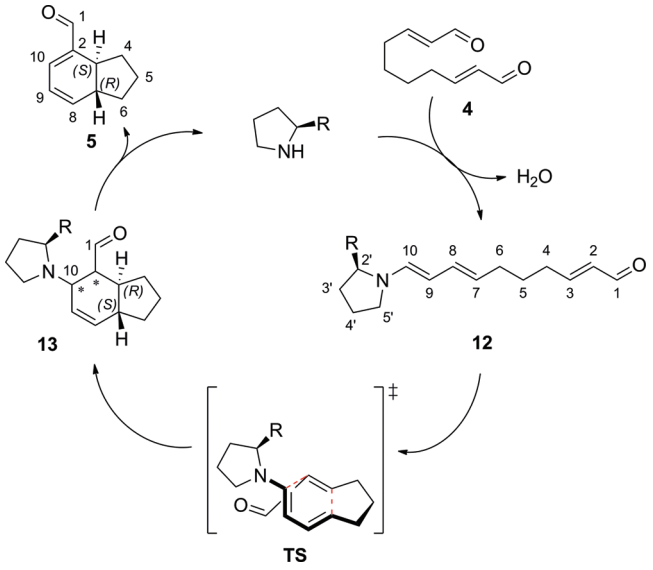

studied over the last years, when the catalyst is proline, and it is now accepted that its carboxylic acid plays an important role in the catalytic process.[23−28] However, the work from Christmann[22] is mainly based on catalysts that do not allow for intramolecular acid catalysis, used alone or assisted by external protic acids, a situation that was not previously studied by computational methods.

Scheme 3. Organocatalytic Intramolecular Diels–Alder Reaction Catalyzed by Chiral Pyrrolidines[22]

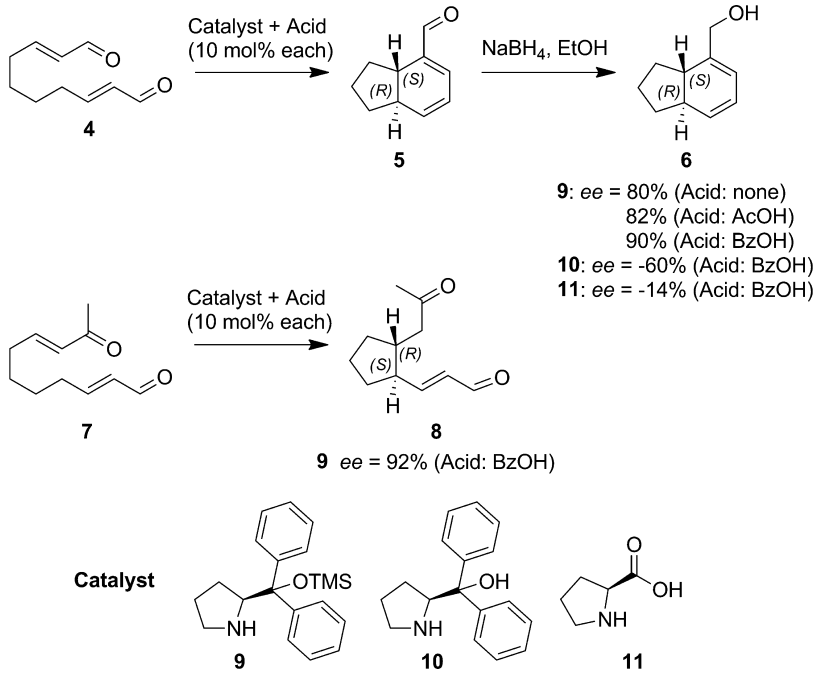

dx.doi.org/10.1021/jo300005e | J. Org. Chem. 2012, 77, 3252–3261

Scheme 5. Enamine Formation in the Presence of an External Protic Acid[a]

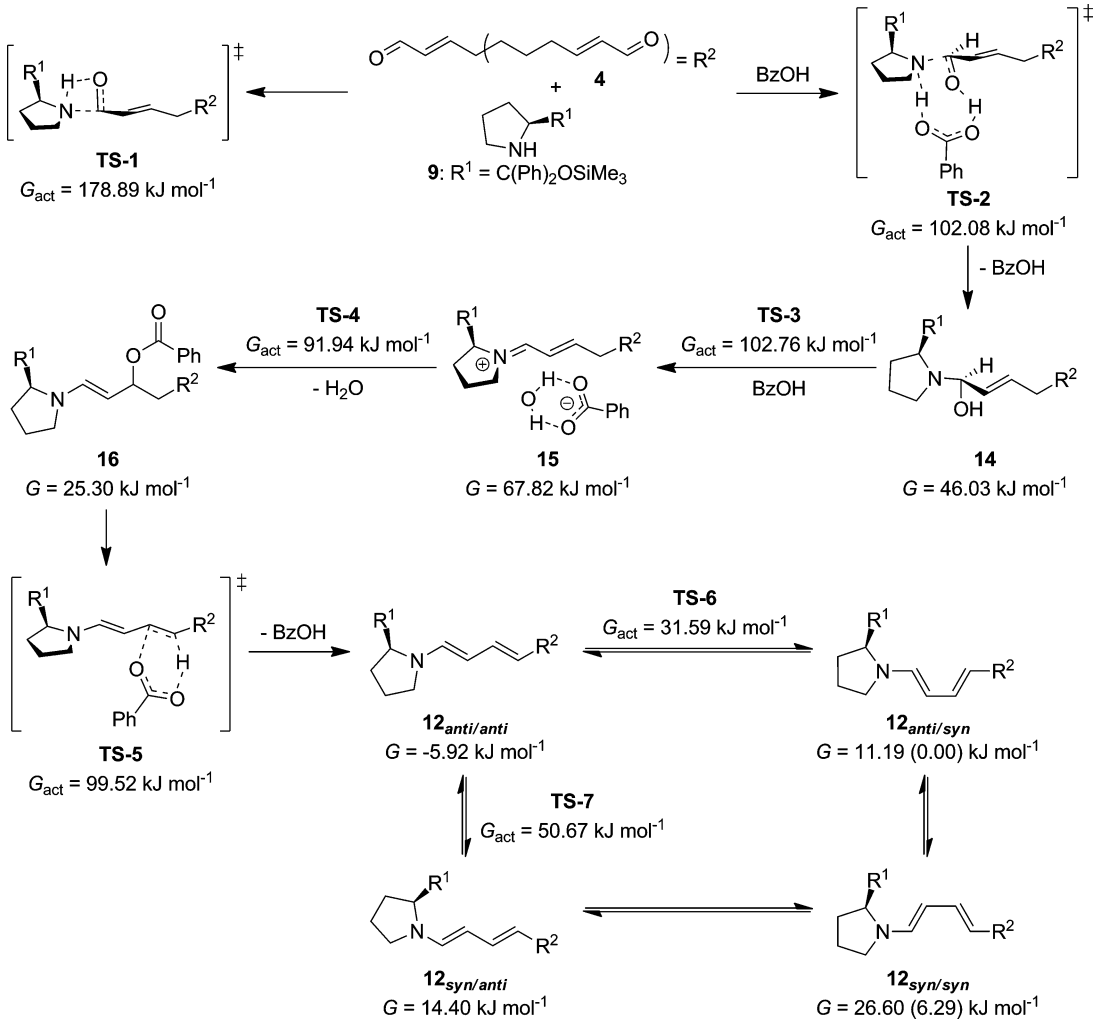

[a]Relative values calculated with M06-2X are shown in parentheses.

In the first step of the enamine formation, an amine has to attack a carbonyl group to originate an α-amino alcohol as a reaction intermediate. However, this process is not possible unless a proton is simultaneously transferred to the carbonyl oxygen atom, thus neutralizing the negative charge that is formed. This proton can be transferred directly from the nitrogen to the oxygen atom, but the activation energy is very high (**TS-1**, G_{act} = 178.9 kJ mol^{-1}, Scheme 5). Proline, or other amine catalysts that can also behave as protic acids, mitigate this problem by protonating the carbonyl group in the TS. An external protic acid as cocatalyst can lead to a similar TS, originating also a strong reduction in the activation energy (**TS-2**, G_{act} = 102.1 kJ mol^{-1}, Scheme 5).

The intermediate formed in the first reaction step has to eliminate water to afford the corresponding iminium salt. When proline is the catalyst, the process is also assisted by its acid group. In the presence of an external protic acid the reaction can proceed by a similar TS (**TS-3**, G_{act} = 102.8 kJ mol^{-1}, Scheme 5), leading to the iminium intermediate **15** in its *anti* configuration. The iminium intermediate is a high energetic species (G = 67.8 kJ mol^{-1}) which, when proline is the catalyst, easily forms a very stable intermediate oxazolidinone ring.[29−31] A similar reaction occurs in the presence of an external carboxylate, leading to intermediate **16**, a species with low relative energy (G = 25.3 kJ mol^{-1}). This structure eliminates the carboxylic acid by a concerted mechanism (**TS-5**, G_{act} = 99.5 kJ mol^{-1}) to form the enamine intermediate **12** in its *anti*/*anti* conformation (Scheme 5). Thus, the three initial steps for the enamine formation are of similar energy in the presence of an external protic acid, while in the absence of acid the reaction rate for the enamine formation shall be much lower, as the activation energy for the first step is ca. 76.8 kJ mol^{-1} higher.

After the dienamine formation, a conformational change has to occur around the C8−C9 carbon bond (Scheme 5), leading to the *s-cis* diene and allowing the IMDA reaction. This conformational change is a fast transformation with low activation energy (**TS-6**, G_{act} = 31.6 kJ mol^{-1}, catalyst **9**). The system can also easily rotate around the C10−N bond (**TS-7**, G_{act} = 50.7 kJ mol^{-1} for catalyst **9**) but the equilibrium is strongly shifted to the *anti* conformation (ΔG = 20.3 kJ mol^{-1}).

As the dieneamine formation does not contribute to the final selectivity, since only one intermediate is formed, and the two conformational changes discussed above are low energy processes, the final selectivity results only from the cyclization step. Thus, the calculation of all relevant transition states involved in this step should give us enough information to allow for a full rationalization of the experimentally observed selectivities.[22]

dx.doi.org/10.1021/jo300005e | J. Org. Chem. 2012, 77, 3252−3261

Table 1. Relative Transition-State Gibbs Energies (kJ mol^{-1}, in Toluene, at Room Temperature) and Enantioselectivities in the IMDA Reaction of Dialdehyde 4 Catalyzed by 9, with and without External Acid

		PBE1PBE/6-311+G**//PBE1PBE/6-31G**					ref 22
transition state		G_{act} (kJ mol^{-1})	ΔG (kJ mol^{-1})	%	ee (%)	de (%)	ee_{exp} (%)
cat. **9**	**TS-8** (*SR*)	68.95	0.00	98.82	99.90	97.74	80 (t = 144 h)[b]
	TS-9 (*RS*)	87.84	18.90	0.05			
	TS-10 (*RR*)	80.03	11.09	1.13	99.92		
	TS-11 (*SS*)	99.25	30.33	0.00			
cat. **9** + BzOH (pK_a = 4.20)	**TS-12** (*SR*)	62.71	0.00	99.05	99.96	98.16	90 (t = 3 h)
	TS-13 (*RS*)	82.22	19.51	0.04			
	TS-14 (*RR*)	74.33	11.62	0.91	99.57		
	TS-15 (*SS*)	89.73	27.02	0.00			
cat. **9** + AcOH (pK_a = 4.76)	**TS-16** (*SR*)	62.78	0.00	99.58	99.93	99.52	82 (t = 12 h)
	TS-17 (*RS*)	82.64	19.86	0.03			
	TS-18 (*RR*)	76.53	13.75	0.39	99.64		
	TS-19 (*SS*)	92.20	29.42	0.00			
cat. **9** HDA[a]	**TS-20** (*SR*)	102.32	3.01	22.87	54.27		
	TS-21 (*RS*)	99.30	0.00	77.13			

[a]HDA − Hetero Diels−Alder. Only one pair of enantiomers was found. [b]50% conversion.

The intramolecular cyclization of dialdehyde **4** leads to intermediate **13**, a structure with four chiral centers (Scheme 4). Thus, intermediate **13** can theoretically be a mixture of 16 stereoisomers, formed via 16 TSs. However, not only does the mechanism discussed in Scheme 5 lead to the trans configuration of both double bonds, but cyclization TSs with *cis* double bonds have considerably higher activation energies, which renders them as low probability structures that do not contribute to the final selectivity. Thus, in this paper we only discuss TSs in which all double bonds have the *trans* configuration.

Intermediate **13** has to eliminate the catalyst to afford structure **5**, a process that reduces the number of asymmetric centers to only two. However this transformation does not reduce the number of transition states needed to be calculated during the cyclization step. After removal of double bond *cis* configurations, the number of TSs becomes dependent only on the type of catalyst, as discussed below. Substituted substrates, that would increase the number of possible diastereomers, are not considered in this discussion, as they did not produce useful regioselectivities.

Christmann used two types of catalysts[22] with or without hydrogen-bond donors (Scheme 3). They originate opposite selectivities and also important differences in the TS structures. We start our discussion with catalyst **9**, a non-hydrogen-bond donor.

The calculated and experimental selectivities obtained with catalyst **9**, in the presence or absence of protic acids, are presented in Table 1, while all relevant TS structures are in Figures 1 (without protic acid) and 2 (explicit addition of protic acid).

Catalyst **9** has a very bulky group that strongly hinders one face of the pyrrolidine ring. Thus, all calculated TSs formed by folding the carbon chain into the same side of the pyrrolidine substituent have very high energy (more than 32 kJ mol^{-1} over **TS-8**, Figure 1). In Figures 1 and 2 only the TSs obtained by folding the carbon chain away of the pyrrolidine substituent are considered.

In the absence of protic acid, the four lowest energy TSs originate two diastereomeric pairs of structure **13** (Scheme 4), which lead to the four possible diastereomers of structure **5** (Scheme 4). Products **5**-*SR* and **5**-*RS* (Scheme 4) derive from

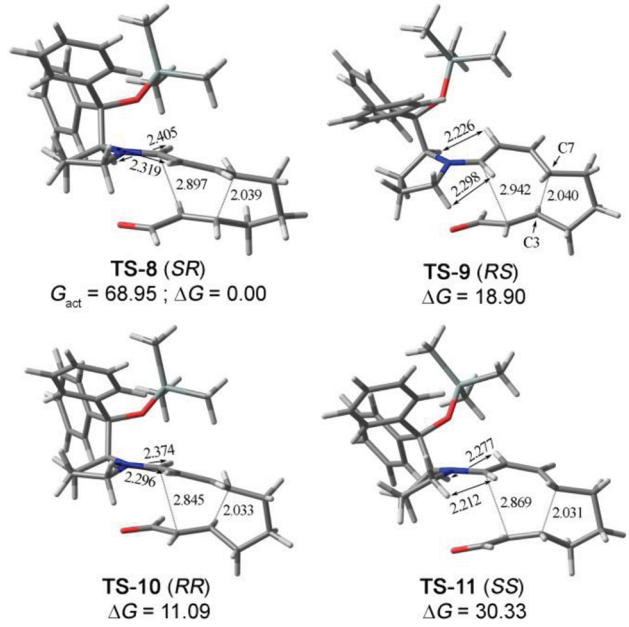

Figure 1. Most stable TS structures for the IMDA reaction of **4** catalyzed by **9**. Relative Gibbs energies in toluene (kJ mol^{-1}). Absolute configurations are attributed only to the chiral centers that remain and are determined in the final products.

transition states **TS-8** and **TS-9**, respectively (Figure 1). The energy difference between **TS-8** and **TS-9** (ΔG = 18.90 kJ mol^{-1}) is mainly caused by the opposite conformations (*anti* vs *syn*) adopted by the TS structures around bond N1′−C1. In the *syn* conformer (**TS-9**), the shorter distance between the large pyrrolidine substituent and the carbon chain originates higher activation energy, a difference that is also observed in intermediate **12** (Scheme 4). **TS-10** (*RR*) and **TS-11** (*SS*) lead to products **5**-*RR* and **5**-*SS*, respectively (Scheme 4). The energy difference calculated between these two isomeric TSs (ΔG = 19.25 kJ mol^{-1}) depends as well on their relative *anti* vs *syn* conformational structures. On the other hand, the diastereoselectivity calculated between the two enantiomeric pairs **TS-8**/**TS-9** and **TS-10**/**TS-11** is mainly originated on the relative configuration of the forming cyclopentane ring, as while

dx.doi.org/10.1021/jo300005e | J. Org. Chem. 2012, 77, 3252−3261

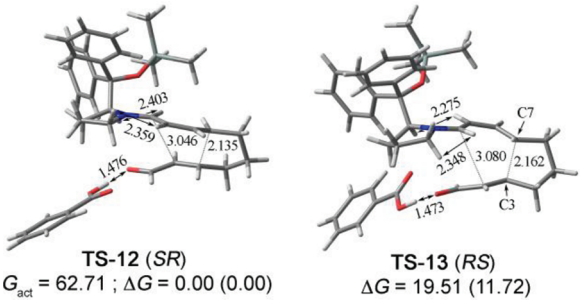

Figure 2. Most stable enantiomeric pair of TS structures for the IMDA reaction of **4** catalyzed by **9** + BzOH. Relative Gibbs energies in toluene (kJ mol^{-1}). Relative values calculated with M06-2X are between parentheses. Absolute configurations are attributed only to the chiral centers that remain and are determined in the final products.

in the first enantiomeric pair the ring susbtituents are in *anti* orientation, in the second enantiomeric pair they are in *syn* orientation. However, and in spite of the good theoretical enantioselectivity calculated for the second enantiomeric pair, due to the large calculated energy difference relative to isomer **TS-8**, we have to conclude that the pair **TS-10**/**TS-11** has to be formed in low amount. Thus, according to our calculations, product **5**-*SR* shall be preferentially formed (via **TS-8**), in agreement with the experimental results. In the following discussion only this enantiomeric pair is considered, but full data is given in the Supporting Information.

Christmann[22] did not observe any product formed by a hetero-DA pathway, in the absence of external protic acid as cocatalyst, as described by Chen.[16] This is in agreement with our results, which indicate that the activation energy for the HDA pathway is considerably higher (Table 1, last entry) than that obtained for the equivalent DA process, indicating that the α,β-unsaturated aldehyde is not enough activated to react as an electron poor diene.

Christmann found that the use of an external protic acid as cocatalyst considerably increases the reaction rate, with a minor improvement in the reaction selectivity (Table 1).[22] As the cyclization step has lower activation energy than the enamine formation steps, we have to conclude that the improvement in the reaction rate results from the reduction of the activation energy in the enamine formation. Thus, the following discussion on the cyclization step with the explicit inclusion of a molecule of cocatalyst as a dienophile activator aims only at the rationalization of its importance in the induction of selectivity (Figure 2 and Table 1).

Transition states **TS-12** to **TS-15** (Table 1) were calculated for the IMDA reaction in the presence of benzoic acid, and it is clear that the transition states with and without acid are very similar structures (Figures 1 and 2). The energy difference between **TS-12** (*SR*) and **TS-13** (*RS*) is similar to that calculated for the pair **TS-8** (*SR*) and **TS-9** (*RS*), thus indicating that the acid only slightly improves the enantioselectivity, in agreement with the experiment. In the presence of benzoic or acetic acids, the Gibbs activation energy decreases by ca. 6.2 kJ mol^{-1} (Table 1), which indicates that while the acid molecule can indeed interact with the dienophile, it only slightly activates the β-carbon (C3) of the aldehyde for the nucleophilic attack of the diene. Thus, the addition of external acid is of minor importance in the cyclization but is mandatory in the enamine formation steps (Scheme 5).

The comparison of the experimental and calculated enantioselectivities presented in Table 1 show a substantial overestimation of the calculated values. This discrepancy with the experiment results from the overestimation of the steric contacts between the pirrolidine substituent and the carbon chain, a result that is already seen in Scheme 5, between the

Table 2. Relative Transition-State Gibbs Energies (kJ mol^{-1}, in Toluene, at Room Temperature) and Enantioselectivities in the IMDA Reaction of Dialdehyde 4 Catalyzed by the Catalysts 9−11 with and without External Acid

		PBE1PBE/6-311+G**//PBE1PBE/6-31G**				ref 22
transition state		G_{act} (kJ mol^{-1})	ΔG (kJ mol^{-1})	%	ee (%)	ee (%)
Cat. **9**	**TS-8** (*SR*)	68.95	0.00	99.95	99.90	80[a] (t = 144 h)
	TS-9 (*RS*)	87.84	18.90	0.05		
Cat. **9** + BzOH	**TS-12** (*SR*)	62.71	0.00	99.96	99.92	90[b] (t = 3 h) 94[c] (48 h)
	TS-13 (*RS*)	82.22	19.51	0.04		
cat. **10**	**TS-22** (*SR*)	85.74	12.98	0.53	−98.79	
	TS-23 (*SR*)	90.54	17.78	0.08		
	TS-24 (*RS*)	72.76	0.00	99.40		
	TS-25 (*RS*)	102.85	30.09	0.00		
cat. **10** + BzOH	**TS-26** (*SR*)	92.36	21.53	0.02	−83.74 −90.97[d]	−60[b] (t = 24 h)
	TS-27 (*SR*)	76.85	6.02	8.11		
	TS-28 (*RS*)	70.84	0.00	91.86		
	TS-29 (*RS*)	94.58	23.75	0.01		
cat. **11**	**TS-30** (*SR*)	68.27	6.49	6.79	−86.43	
	TS-31 (*SR*)	95.38	33.60	0.00		
	TS-32 (*RS*)	61.78	0.00	93.21		
	TS-33 (*RS*)	95.62	33.84	0.00		
cat. **11** + BzOH	**TS-34** (*SR*)	69.77	4.50	14.01	−71.94 −78.89[d]	−14[a,b](t = 22 h)
	TS-35 (*SR*)	86.33	21.05	0.02		
	TS-36 (*RS*)	65.27	0.00	85.97		
	TS-37 (*RS*)	91.58	26.31	0.00		

[a]50% conversion. [b]Acidic conditions, BzOH. [c]In CH_2Cl_2 at −18 °C. [d]Values calculated by Boltzmann averaging of the two processes with and without protic acid participation.

dx.doi.org/10.1021/jo300005e | J. Org. Chem. 2012, 77, 3252−3261

reacting conformers $\mathbf{12}_{anti/syn}$ and $\mathbf{12}_{syn/syn}$. The use of M06-2X (Figure 2 and Scheme 5) reduces the overestimation, thus leading to quite better agreement between the calculated and the experimental data. A similar conclusion is obtained if wB97XD is used (see the Supporting Information).

Christmann has also tested hydrogen-bond-donor catalysts **10** and **11**.[22] The result is quite interesting, as inversion of configuration was obtained in both cases (Table 2). Thus, with dialdehyde **4** as substrate, while catalyst **9** (Scheme 3), a non-hydrogen-bond donor, induces an ee of 90%, catalyst **10**, with a free hydroxyl group, induces an ee of −60% and proline (**11**) induces an ee of −14% (Table 2). No experimental results with catalysts **9** and **10** are available in the absence of external protic acid, but we shall discuss both possibilities (with and without acid) in order to evaluate its importance in the cyclization step, when these two catalysts are used.

As discussed before, catalyst **9** only allows one low energy fold of the carbon chain in the cyclization TSs. In the case of catalysts **10** and **11**, two opposite folds are possible, into the same side of the pyrrolidine substituent or into the opposite side. Both possibilities were considered, and the results are in Table 2 and Figures 3 (catalyst **10**) and 4 (proline, **11**).

By comparison with the results obtained for catalyst **9** in the absence of protic acid, the lowest energy TSs resulting from the folds at the opposite side of the pyrrolidine ring substituent are more energetic in ca. 30 kJ mol^{-1} when catalyst **10** is used and in ca. 34 kJ mol^{-1} when proline (**11**) is the catalyst. The fold at the same side of the pyrrolidine substituent, which allows for the establishment of hydrogen bonds between the catalyst substituent and the carbonyl oxygen atom in the side chain, raises the activation energy by ca. 4 kJ mol^{-1} for catalyst **10** and decreases the activation energy by ca. 7 kJ mol^{-1} for proline (**11**) (energy differences by comparison with the energy of structure **TS-8**, Figure 1). These differences indicate that the existence of the silyloxy group in the catalyst is very important for the activation of the diene, as the attacks at the opposite side of the pyrrolidine substituent are more energetic for catalysts **10** and **11**. The formation of a hydrogen bond between the acid group and the nitrogen atom in proline (Figure 3) also contributes to the increase of the activation energy, as the electro-donation ability of the diene is reduced. On the other hand, the stronger acidity of proline is enough to reduce the activation energy of **TS-32**, in comparison with **TS-8**, by strongly activating the dienophile. Thus, the lowest energy TSs calculated for both catalysts **10** and **11**, in the absence of external acid, are those in which the dialdehyde chain folds into the side of the pyrrolidine substituent, allowing for the establishment of hydrogen bonds and leading to the induction of inverse selectivity (compared with catalyst **9**). The reasons for the calculated selectivity are similar to those discussed for catalyst **9**. The enantioselectivity results from the *syn*/*anti* orientation around the C−N bond, while the diastereoselectivity mainly results from the *syn*/*anti* configuration of the substituents in the forming cyclopentane ring.

The experimental results for catalysts **10** and **11** were obtained with benzoic acid as cocatalyst.[22] Table 2 and Figures 3 and 4 show the calculated results when a molecule of benzoic acid is explicitly considered in the TS structures, indicating that while the acid reduces the activation energy of some TSs and raises others, it slightly erodes the calculated selectivities for both catalysts, leading to better agreement with the experimental results.

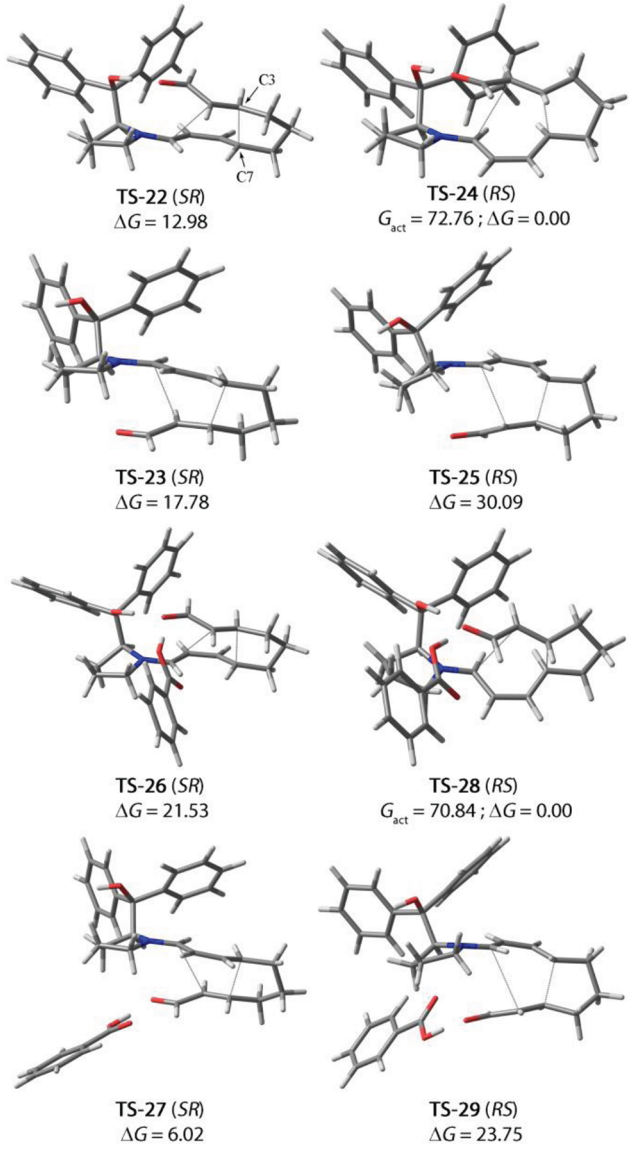

Figure 3. Most stable enantiomeric pair of TS structures for the IMDA reaction of **4**, with two possible orientations of the carbon chain, catalyzed by **10** with and without benzoic acid. Relative Gibbs energies in toluene (kJ mol^{-1}). Absolute configurations are attributed only to the chiral centers that remain and are determined in the final products.

According to the results from Christmann,[22] the structure of the dialdehyde can dramatically change the reaction outcome. Thus, it was observed that while dialdehyde **17** cyclizes to structure **19** (*SR*) with yield and selectivity similar to those found in the cyclization of **4**, dialdehyde **18** does not react, but nothing is said on the recovery of starting material or its reaction to originate other products (Scheme 6).

Table 3 shows the calculated activation energies for the cyclization of **17** and **18** catalyzed by **9** alone or in the presence of benzoic acid as cocatalyst. The energetic values suggest that both compounds **17** and **18** should form products with similar selectivities, indicating that the size of the carbon chain is not very important in this respect. However, they also clearly indicate that while **17** and **4** have very similar activation energies for the cyclization ($\Delta G_{act\ (acid)}$ = 6.5 kJ mol^{-1}), the cyclization of **18** occurs via a TS structure with a larger value ($\Delta G_{act\ (acid)}$ = 47.5 kJ mol^{-1}). This difference renders **18** much

dx.doi.org/10.1021/jo300005e | J. Org. Chem. 2012, 77, 3252−3261

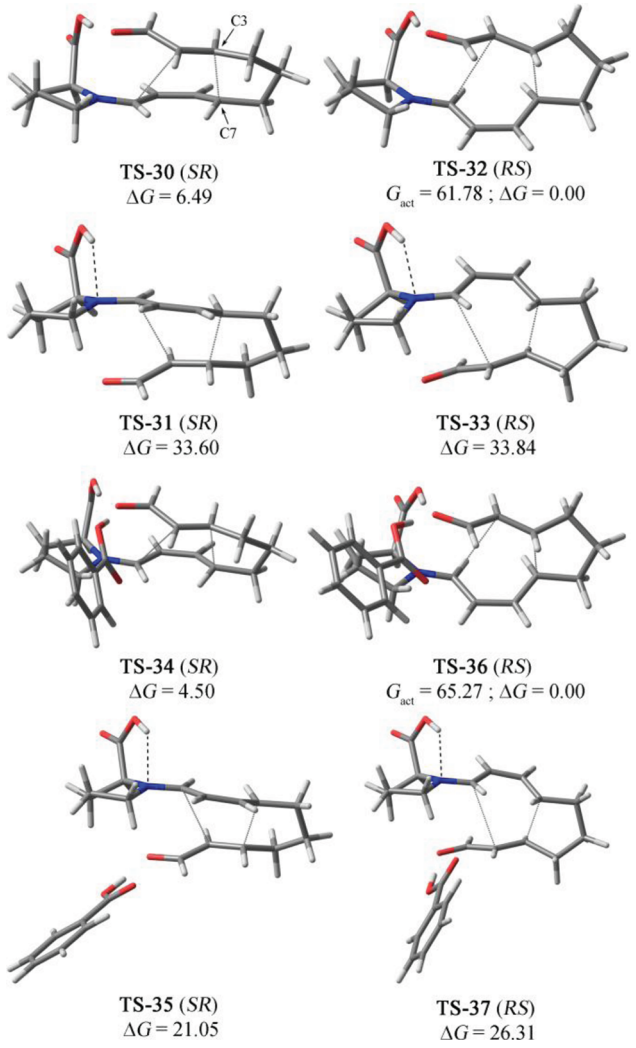

Figure 4. Most stable enantiomeric pair of TS structures for the IMDA reaction of **4**, with two possible orientations of the carbon chain, catalyzed by **11** with and without benzoic acid. Relative Gibbs energies in toluene (kJ mol^{-1}). Absolute configurations are attributed only to the chiral centers that remain and are determined in the final products.

Scheme 6. Organocatalytic Intramolecular Diels–Alder Reaction of Compounds 17 and 18[22]

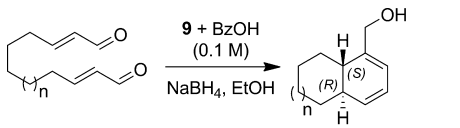

less reactive in the reaction conditions, as the experiment shows.

The experiment also shows[22] that the α-methylene aldehyde **21** (Scheme 7) reacts to form compound **26**, possibly by an *exo*-aldol mechanism. The DA mechanism is not possible in this case, as it would lead to a four-membered ring TS (we were not able to find a TS for the DA reaction). However, this compound can also react by HDA, Michael, or Mannich pathways, as all of them lead to five-membered ring systems. We studied all these possibilities and found that the HDA process is also improbable, as its activation energy is ca. 30 kJ mol^{-1} higher than the *exo*-aldol pathway. The *endo*-Michael

Table 3. Relative Transition-State Gibbs Energies (kJ mol^{-1}, in Toluene, At Room Temperature) and Enantioselectivities in the IMDA Reaction of Dialdehydes 17 and 18 Catalyzed by 9, with and without Benzoic Acid as Cocatalyst

			PBE1PBE/6-311+G**//PBE1PBE/6-31G**				ref 22
transition state			G_{act} (kJ mol^{-1})	ΔG (kJ mol^{-1})	%	ee (%)	ee$_{exp}$ (%)	G_{act} (kJ mol^{-1})
17	cat. **9**	**TS-38** (*SR*)	77.89	0.00	99.93	99.86		
		TS-39 (*RS*)	95.87	17.99	0.07			
	cat. **9** + BzOH	**TS-40** (*SR*)	69.19	0.00	99.99	99.98		95
		TS-41 (*RS*)	91.87	22.69	0.01			
18	cat. **9**	**TS-42** (*SR*)	120.13	0.00	99.96	99.92		
		TS-43 (*RS*)	139.64	19.51	0.04			
	cat. **9** + BzOH	**TS-44** (*SR*)	110.17	0.00	99.81	99.63		
		TS-45 (*RS*)	125.74	15.57	0.19			

mechanism, which leads to product **24**, has an activation energy ca. 23 kJ mol^{-1} higher than that calculated for the enol pathway, indicating that it should not be followed, in agreement with the experiment. The Mannich pathway leads also to compound **26** but shows that the initial attack of the amine catalyst occurs at the C1 carbon atom, with formation of the corresponding iminium salt. As the enamine formation is the rate-limiting step for the aldol pathway, our results suggest that the Mannich reaction cannot be responsible for the formation of product **26**, since the activation energy for the amine attack at C1 is 14.5 kJ mol^{-1} higher than the similar attack at C8 (TS-46 vs TS-47, Scheme 7). Thus, the conclusion is that product **26** is formed via the *exo*-aldol pathway, in agreement with the suggestion of Christmann[22] and Baldwin's rules.[32−34]

The experimental result obtained for ketoaldehyde **7** (Scheme 8) is quite interesting, as no formal DA reaction is observed in this case.[22] Instead, an apparent direct enantioselective vinylgous Michael addition leads to ketoaldehyde **8** (Scheme 8).

According to our calculations, in acidic conditions both the intramolecular Michael addition and the IMDA reaction pathways can be followed (Scheme 8). However, the Michael reaction has higher activation energy than the IMDA pathway (ca. 10 kJ mol^{-1}) and leads to low and inverted selectivity (ee$_{(SR/RS)}$ = -6.2%) relative to the experimental value (ee$_{(SR/RS)}$ = 92%). On the other hand, the IMDA pathway predicts the proper selectivity (ee = 99.96%, Table 1) but does not explain the formation of the Michael adduct. Interestingly, the Boltzmann averaging of the selectivities obtained considering the participation of both pathways leads to an ee = 95.42%, well in agreement with the experimental value. Thus, the experimental results can be explained if we find a reason to justify the ring-opening of intermediate **30**, followed by conventional iminium hydrolysis, and average the selectivities obtained in the two concurrent Michael and DA pathways.

In Scheme 9 we compare the energetics for catalyst elimination vs ring-opening pathways for the cyclized intermediates originating from dialdehyde **4** and ketoaldehyde **7**. It is clear that while intermediate **32** (resulting from the dialdehyde cyclization) preferentially eliminates the catalyst and

dx.doi.org/10.1021/jo300005e | J. Org. Chem. 2012, 77, 3252−3261

Scheme 7. Possible Reaction Pathways for the Treatment of the α-Methylene Aldehyde 21 with Catalyst 9

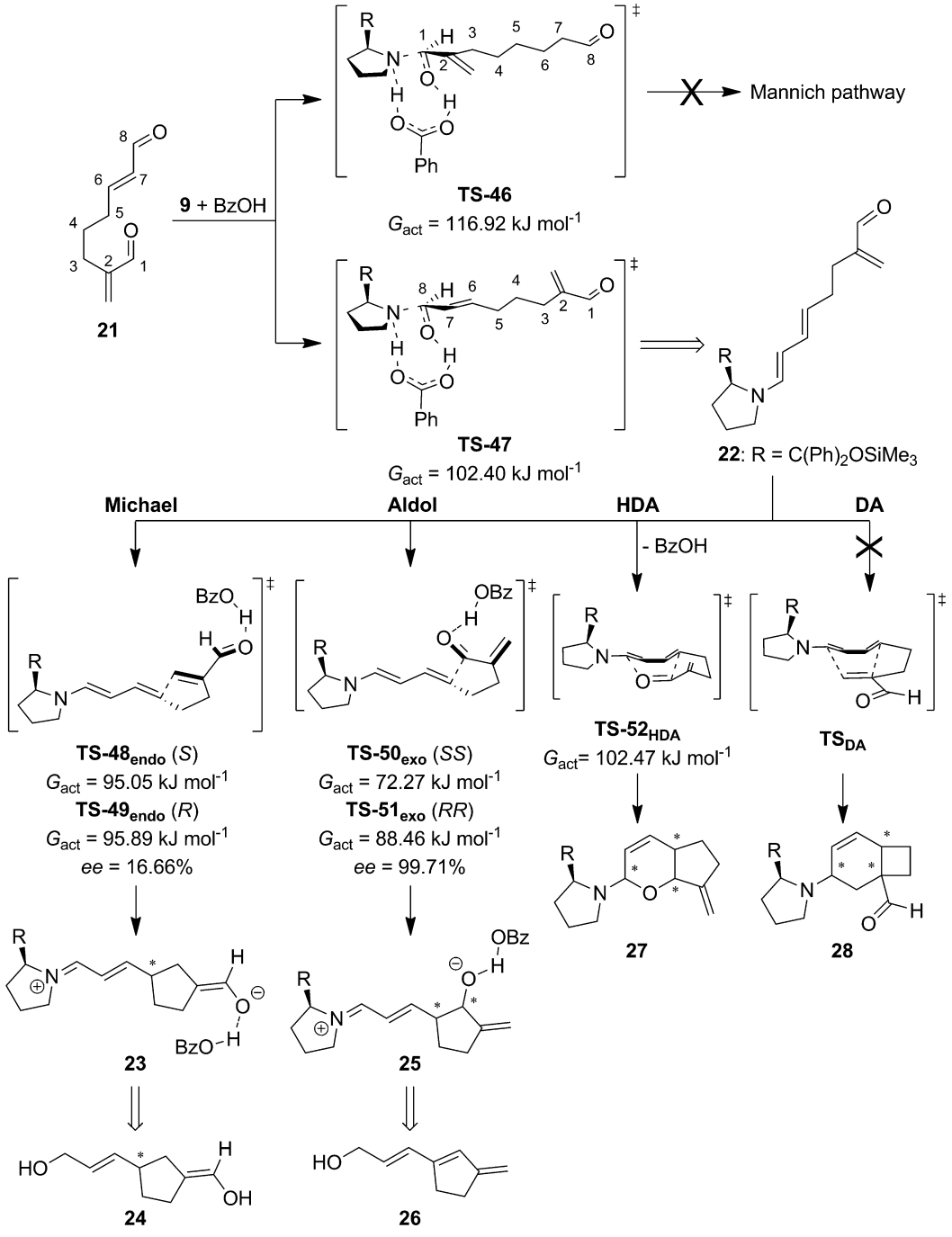

leads to product **5** (ΔG = 50.4 kJ mol^{-1} for **TS-62** vs ΔG = 68.7 kJ mol^{-1} for **TS-57**), intermediate **31** (resulting from the ketoaldehyde cyclization) can undergo a ring-opening process (ΔG = 76.9 kJ mol^{-1} for **TS-58**) as easily as the catalyst elimination (ΔG = 74.9 kJ mol^{-1} for **TS-63**). Thus, statistical factors, such as the low concentration of free amine, can make the catalyst elimination less probable, resulting in a preferential ring-opening pathway. Carboxylate anion can add to the iminium intermediate **30** with no activation energy, which catalyzes the double-bond isomerization (**TS-59**). In the following steps, the iminium intermediate undergoes acid-catalyzed hydrolysis via low activation energy transition states (see the Supporting Information for a full analysis), which results in the final Michael product **8**. The reaction pathway proposed in Scheme 9 was further verified by other theoretical methods (B3LYP, PBEh1PBE, and M06-2X; see the Supporting Information).

■ CONCLUSIONS

The experimental diastereoselectivity obtained in amine-catalyzed intramolecular Diels–Alder reactions of α,β-unsaturated carbonylic compounds was for the first time theoretically rationalized. We found that with amine catalysts lacking a carboxylic or hydroxylic function, the use of an external protic acid is mandatory both in the initial enamine formation steps and in the final catalyst elimination, while it marginally influences the cyclization step. Thus, while the overall reaction rate is determined by the enamine formation, the enantiose-

dx.doi.org/10.1021/jo300005e | J. Org. Chem. 2012, 77, 3252–3261

Scheme 8. Proposed Mechanisms for the Formation of Michael Products, in the Treatment of Ketoaldehyde 7 with Catalyst 9, in the Presence of Benzoic Acid

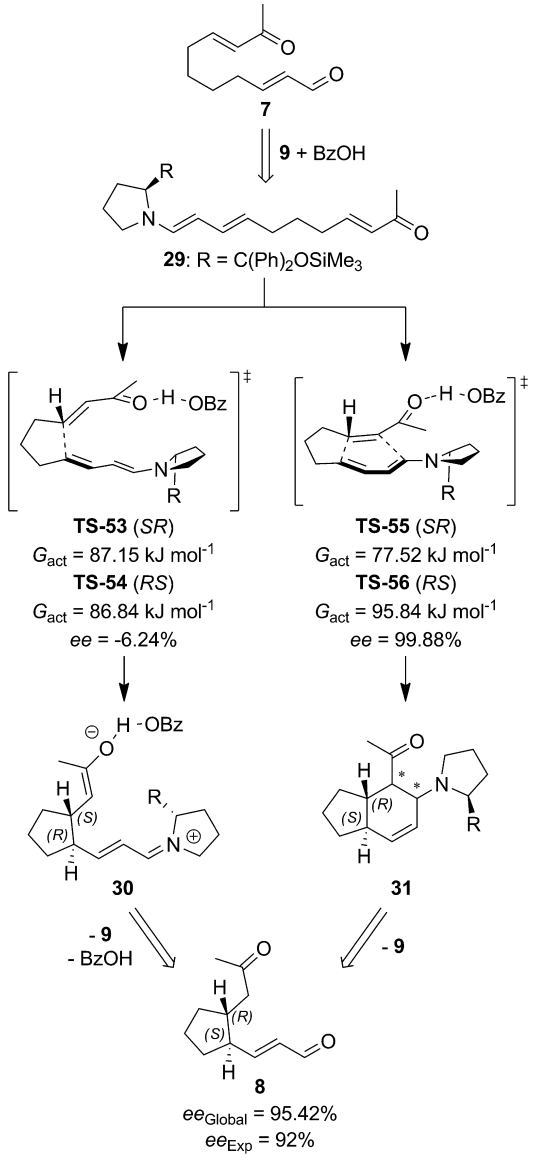

lectivity results from the *syn*/*anti* orientation around the C−N enamine bond in the cyclization step. The diastereoselectivity is also induced in this step, due to the *syn*/*anti* configuration of the substituents in the forming cyclopentane ring. When proline or other hydrogen-bond-donor catalysts are used, the selectivity can be explained by the hydrogen bond that is formed in the cyclization TSs, resulting in inverted configuration and lower selectivity. The different behavior between dialdehydes and ketoaldehydes is proposed to be resulting from different reaction rates in the final catalyst elimination step.

COMPUTATIONAL METHODS

Full geometry optimizations have been performed with the Gaussian 09, Revision B.01, suite of programs[35] employing density functional theory (DFT)[36,37] with the hybrid functional PBE1PBE[38−41] and the 6-31G** basis set. Harmonic vibrational frequencies have been calculated for all located stationary structures to verify whether they are minima or transition states. Zero-point energies and thermal corrections have been taken from unscaled vibrational frequencies.

Scheme 9. Proposed Mechanism for the Formation of a Michael Product via the DA Cyclization Pathway

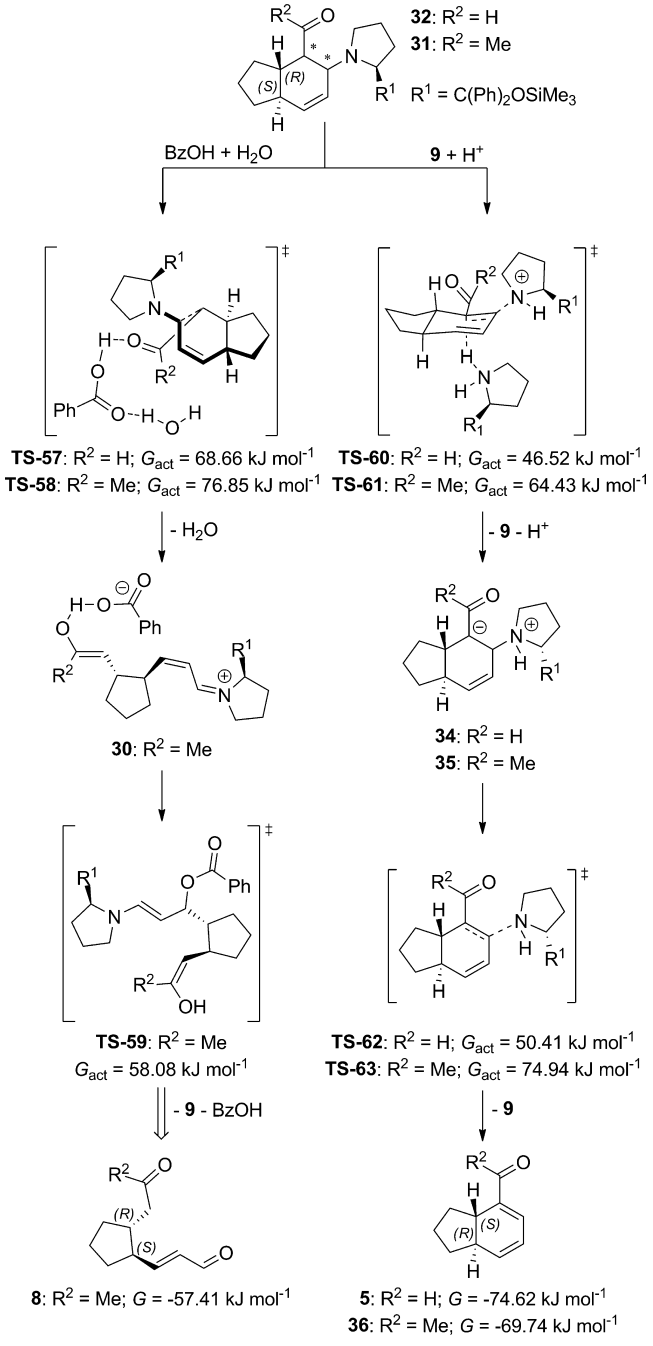

Free energies of activation, unless otherwise stated, are given at 25 °C. The energy values have been refined by single point DFT calculations at the PBE1PBE/6-311+G** level of theory, over the optimized gas-phase geometries. All structures in Scheme 9 were also calculated with B3LYP,[42,43] PBEh1PBE,[44] and M06-2X,[45] and selected structures in Scheme 5 and Figure 2 were also calculated with M06-2X and wB97XD[46] (see the Supporting Information). Solvent effects in toluene have been taken in account by single-point calculations with the polarizable continuum model (PCM)[47] over the respective gas-phase geometries. All energies are calculated relative to the reagents. All bond lengths are in angstroms (Å) and energies in kJ mol^{-1}.

dx.doi.org/10.1021/jo300005e | J. Org. Chem. 2012, 77, 3252−3261

■ ASSOCIATED CONTENT

Supporting Information

Cartesian coordinate matrixes and electronic energies of all calculated structures. This material is available free of charge via the Internet at http://pubs.acs.org.

■ AUTHOR INFORMATION

Corresponding Author

*E-mail: ags@fct.unl.pt.

Notes

The authors declare no competing financial interest.

■ ACKNOWLEDGMENTS

We are grateful to the Fundação para a Ciência e Tecnologia (PTDC/QUI-QUI/104056/2008) for financial support.

■ REFERENCES

(1) Kagan, H. B.; Riant, O. *Chem. Rev.* **1992**, *92*, 1007.
(2) Corey, E. J. *Angew. Chem., Int. Ed.* **2002**, *41*, 1650.
(3) Reymond, S.; Cossy, J. *Chem. Rev.* **2008**, *108*, 5359.
(4) Merino, P.; Marques-Lopez, E.; Tejero, T.; Herrera, R. P. *Synthesis* **2010**, *1*, 1.
(5) Ahrendt, K. A.; Borths, C. J.; MacMillan, D. W. C. *J. Am. Chem. Soc.* **2000**, *122*, 4243.
(6) Jen, W. S.; Wiener, J. J. M.; MacMillan, D. W. C. *J. Am. Chem. Soc.* **2000**, *122*, 9874.
(7) Paras, N. A.; MacMillan, D. W. C. *J. Am. Chem. Soc.* **2001**, *123*, 4370.
(8) Austin, J. F.; MacMillan, D. W. C. *J. Am. Chem. Soc.* **2002**, *124*, 1172.
(9) Brown, S. P.; Goodwin, N. C.; MacMillan, D. W. C. *J. Am. Chem. Soc.* **2003**, *125*, 1192.
(10) Ouellet, S. G.; Tuttle, J. B.; MacMillan, D. W. C. *J. Am. Chem. Soc.* **2005**, *127*, 32.
(11) Bertelsen, S.; Marigo, M.; Brandes, S.; Diner, P.; Jorgensen, K. A. *J. Am. Chem. Soc.* **2006**, *128*, 12973.
(12) Juhl, K.; Jorgensen, K. A. *Angew. Chem., Int. Ed.* **2003**, *42*, 1498.
(13) He, M.; Struble, J. R.; Bode, J. W. *J. Am. Chem. Soc.* **2006**, *128*, 8418.
(14) Han, B.; He, Z. Q.; Li, J. L.; Li, R.; Jiang, K.; Liu, T. Y.; Chen, Y. C. *Angew. Chem., Int. Ed.* **2009**, *48*, 5474.
(15) Xie, M. S.; Chen, X. H.; Zhu, Y.; Gao, B.; Lin, L. L.; Liu, X. H.; Feng, X. M. *Angew. Chem., Int. Ed.* **2010**, *49*, 3799.
(16) Li, J. L.; Kang, T. R.; Zhou, S. L.; Li, R.; Wu, L.; Chen, Y. C. *Angew. Chem., Int. Ed.* **2010**, *49*, 6418.
(17) Lygo, B.; Bhatia, M.; Cooke, J. W. B.; Hirst, D. J. *Tetrahedron Lett.* **2003**, *44*, 2529.
(18) Wilson, R. M.; Jen, W. S.; MacMillan, D. W. C. *J. Am. Chem. Soc.* **2005**, *127*, 11616.
(19) Burns, A. C.; Forsyth, C. J. *Org. Lett.* **2008**, *10*, 97.
(20) de Figueiredo, R. M.; Berner, R.; Julis, J.; Liu, T.; Tuerp, D.; Christmann, M. *J. Org. Chem.* **2007**, *72*, 640.
(21) Chackalamannil, S.; Davies, R. J.; Wang, Y.; Asberom, T.; Doller, D.; Wong, J.; Leone, D.; McPhail, A. T. *J. Org. Chem.* **1999**, *64*, 1932.
(22) de Figueiredo, R. M.; Frohlich, R.; Christmann, M. *Angew. Chem., Int. Ed.* **2008**, *47*, 1450.
(23) Clemente, F. R.; Houk, K. N. *Angew. Chem., Int. Ed.* **2004**, *43*, 5766.
(24) Duarte, F. J. S.; Cabrita, E. J.; Frenking, G.; Santos, A. G. *Chem.—Eur. J* **2009**, *15*, 1734.
(25) Duarte, F. J. S.; Cabrita, E. J.; Frenking, G.; Santos, A. G. *J. Org. Chem.* **2010**, *75*, 2546.
(26) Nielsen, M.; Worgull, D.; Zweifel, T.; Gschwend, B.; Bertelsen, S.; Jorgensen, K. A. *Chem. Commun.* **2011**, *47*, 632.
(27) Cheong, P. H.-Y.; Legault, C. Y.; Um, J. M.; Çelebi -Ölçüm, N.; Houk, K. N. *Chem. Rev.* **2011**, *111*, 5042.
(28) Moyano, A.; Rios, R. *Chem. Rev.* **2011**, *111*, 4703.
(29) Seebach, D.; Beck, A. K.; Badine, D. M.; Limbach, M.; Eschenmoser, A.; Treasurywala, A. M.; Hobi, R.; Prikoszovich, W.; Linder, B. *Helv. Chim. Acta* **2007**, *90*, 425.
(30) Gschwind, R. M.; Schmid, M. B.; Zeitler, K. *Angew. Chem., Int. Ed.* **2010**, *49*, 4997.
(31) Ajitha, M. J.; Suresh, C. H. *J. Mol. Catal. A: Chem* **2011**, *345*, 37.
(32) Baldwin, J. E. *J. Chem. Soc., Chem. Commun.* **1976**, 734.
(33) Baldwin, J. E.; Thomas, R. C.; Kruse, L. I.; Silberman, L. *J. Org. Chem.* **1977**, *42*, 3846.
(34) Johnson, C. D. *Acc. Chem. Res.* **1993**, *26*, 476.
(35) Gaussian 09, Rev. B.01: Frisch, M. J.; Trucks, G. W.; Schlegel, H. B.; Scuseria, G. E.; Robb, M. A.; Cheeseman, J. R.; Scalmani, G.; Barone, V.; Mennucci, B.; Petersson, G. A.; Nakatsuji, H.; Caricato, M.; Li, X.; Hratchian, H. P.; Izmaylov, A. F.; Bloino, J.; Zheng, G.; Sonnenberg, J. L.; Hada, M.; Ehara, M.; Toyota, K.; Fukuda, R.; Hasegawa, J.; Ishida, M.; Nakajima, T.; Honda, Y.; Kitao, O.; Nakai, H.; Vreven, T.; Montgomery, J. A., Jr.; Peralta, J. E.; Ogliaro, F.; Bearpark, M.; Heyd, J. J.; Brothers, E.; Kudin, K. N.; Staroverov, V. N.; Kobayashi, R.; Normand, J.; Raghavachari, K.; Rendell, A.; Burant, J. C.; Iyengar, S. S.; Tomasi, J.; Cossi, M.; Rega, N.; Millam, J. M.; Klene, M.; Knox, J. E.; Cross, J. B.; Bakken, V.; Adamo, C.; Jaramillo, J.; Gomperts, R.; Stratmann, R. E.; Yazyev, O.; Austin, A. J.; Cammi, R.; Pomelli, C.; Ochterski, J. W.; Martin, R. L.; Morokuma, K.; Zakrzewski, V. G.; Voth, G. A.; Salvador, P.; Dannenberg, J. J.; Dapprich, S.; Daniels, A. D.; Ö. Farkas, Foresman, J. B.; Ortiz, J. V.; Cioslowski, J.; Fox, D. J. Gaussian, Inc., Wallingford. CT, 2009.
(36) Koch, W.; Holthausen, M. C. *A Chemist's Guide to Density Functional Theory*, 2nd ed.; Wiley: New York, 2001.
(37) Parr, R. G.; Yang, W. *Density Functional Theory of Atoms and Molecules*; Oxford University Press: Oxford, 1989.
(38) Perdew, J. P.; Burke, K.; Ernzerhof, M. *Phys. Rev. Lett.* **1996**, *77*, 3865.
(39) Perdew, J. P.; Burke, K.; Ernzerhof, M. *Phys. Rev. Lett.* **1997**, *78*, 1396.
(40) Adamo, C.; Barone, V. *J. Chem. Phys.* **1999**, *110*, 6158.
(41) Wheeler, S. E.; Moran, A.; Pieniazek, S. N.; Houk, K. N. *J. Phys. Chem. A* **2009**, *113*, 10376.
(42) Becke, A. D. *J. Chem. Phys.* **1993**, *98*, 5648.
(43) Lee, C.; Yang, W.; Parr, R. G. *Phys. Rev. B* **1988**, *37*, 785.
(44) Ernzerhof, M.; Perdew, J. P. *J. Chem. Phys.* **1998**, *109*, 3313.
(45) Zhao, Y.; Truhlar, D. G. *Theor. Chem. Acc.* **2008**, *120*, 215.
(46) Chai, J.-D.; Head-Gordon, M. *Phys. Chem. Chem. Phys.* **2008**, *10*, 6615.
(47) Tomasi, J.; Mennucci, B.; Cammi, R. *Chem. Rev.* **2005**, *105*, 2999−3093.